ALPHA DECAY AND VERY ASYMMETRIC SPONTANEOUS FISSION

G. ROYER

Rapport Interne SUBATECH 00-02

Alpha decay and very asymmetric spontaneous fission

G. Royer [1]

Laboratoire Subatech, UMR: IN2P3/CNRS-Université-Ecole des Mines, 4 rue A. Kastler, 44307 Nantes Cedex 03, France

Abstract

Regarding the α decay as a spontaneous very asymmetric fission, the α emission half-lives have been calculated within the WKB barrier penetration probability and without preformation factor. The potential energy has been calculated within a liquid drop model including the proximity effects between the α particle and the daughter nucleus and adjusted to reproduce the experimental Q_α. For 373 α emitters, the rms deviation between the theoretical and experimental values of $log_{10}[T_{1/2}(s)]$ is only 0.63. Predictions for the heaviest and super heavy elements are presented as well as simple analytical formulas for $log_{10}[T_{1/2}(s)]$.

PACS: 23.60.+e; 21.60.Ev; 24.75.+i; 27.90.+b
Keywords: α decay; Half-lives; Liquid drop model; Asymmetric fission, Superheavy elements

[1] E-mail:royer@subatech.in2p3.fr

1 Introduction

The synthesis of very heavy elements has strongly advanced recently [1–5] and their half-lives, decay modes and mass will test the ideas developed over more than 30 years on the structure of nuclei with a large number of protons and neutrons. The main and often the only observed decay mode of these heaviest systems is the α emission. In this mass range, it was not expected that the α decay was so competitive in regard to the spontaneous fission.

In addition to the interest in searching for the alpha-decay chains of the super heavy elements, the alpha decay data have been also recently used to obtain important informations on the spectroscopy of very neutron deficient nuclei [6] and mass surface close to the drip line. The branching ratio of the C, O, Ne, Mg and Si emission by heavy nuclei, the so-called cluster radioactivity, is also given relatively to the α emission [7].

The α decay was firstly described in 1928 [8,9] within a quantum tunneling through the potential barrier leading from the mother nucleus to the two emitted fragments: the α particle and the daughter nucleus. The spontaneous fission discovered later and the cluster radioactivity observed from 1984 are fundamentally also quantum tunneling processes through the decay barrier. The open question is whether these three decay modes correspond to the fission of a nuclear liquid drop but for three very different mass asymmetries or the alpha and cluster radioactivities are exit channels distinct from the fission one and correspond to the emission of preformed clusters. In the unified fission approaches [10,11] the decay constant λ is simply the product of the barrier penetrability P and of a constant assault frequency ν_0. Then, the height, position and width of the potential barriers are the main ingredients determining the half-lives. In the preformed cluster models [12], the decay constant is the product of three terms : the barrier penetrability P, the assault frequency ν_0 and the cluster preformation probability P_0, the two last contributions varying with the size of the preformed cluster.

Fusion studies [13,14] have clearly demonstrated that the height of the pure Coulomb barrier at the contact point does not reproduce the experimental fusion barrier heights. When two nuclei are close, a proximity energy must be added to take into account the nuclear interaction forces. For the three discussed decay modes, the importance of the one-body shapes decreases with asymmetry and, for the α decay, the path leading from the mother nucleus till the touching configuration is only a very small part of the potential barrier when the proximity is introduced. Consequently, for the α emission, the difference between the asymmetric fission approaches and the preformed cluster models appears essentially in the way to determine the decay constant rather in the choice of the shape sequence or potential energy before the rupture of

the neck between the fragments.

The purpose of the present work is firstly to study to what extent the generalized liquid drop model (GLDM) and the quasi-molecular shapes which have allowed to reproduce reasonably most of the fusion, fission and cluster radioactivity data [11,14–16] are also able to reproduce the α decay barrier and then the half-lives using the experimental Q_α and without introducing any new artificial adjustable parameter. Obtaining an over-all agreement, predictions for the α decay half-lives of the heaviest and super heavy systems are presented from theoretical Q_α. Since the Geiger and Nutall plots [17] several expressions have been advanced for $log_{10}[T_{1/2}(s)]$ [18–21]. New simple analytical formulas fitted on a set of 373 alpha emitters are again proposed here.

2 Asymmetric fission model

The main part of the α decay barrier corresponds to two separated nuclei and the distance r between their centres of mass has been taken as the deformation parameter. The selected shape to describe the one-body configurations before the separation plays only a minor role and the shape sequence already used to describe the asymmetric fusion and fission [13,14] has been kept. Therefore, the future α particle and daughter nucleus are portions of lemniscatoids joined on a plane perpendicular to the fission axis. This implicitly supposes that the α particle is formed at the surface of the mother nucleus without preformation.

The effective sharp radius of the radioactive emitter is defined by

$$R_0 = 1.28A^{1/3} - 0.76 + 0.8A^{-1/3}\ fm. \tag{1}$$

This formula allows to reproduce the increase of the ratio $r_0 = R_0/A^{1/3}$ with the mass; for example, r_0=1.11 fm for ^{20}Ne, 1.16 fm for ^{108}Te and 1.18 fm for ^{264}Hs.
To ensure volume conservation, the radii R_d and R_α of the daughter and alpha nuclei are given by

$$R_d = R_0(1+\beta^3)^{-1/3}, R_\alpha = R_0\beta(1+\beta^3)^{-1/3}, \tag{2}$$

where

$$\beta = \frac{1.28A_\alpha^{1/3} - 0.76 + 0.8A_\alpha^{-1/3}}{1.28A_d^{1/3} - 0.76 + 0.8A_d^{-1/3}}. \tag{3}$$

After the separation, the volume, surface and Coulomb energies of the GLDM

read

$$E_V = -15.494[(1 - 1.8I_d^2)A_d + A_\alpha]\ MeV, \tag{4}$$

$$E_S = 17.9439[(1 - 2.6I_d^2)A_d^{2/3} + A_\alpha^{2/3}]\ MeV, \tag{5}$$

$$E_C = 0.6e^2 Z_d^2/R_d + 0.6e^2 Z_\alpha^2/R_\alpha + e^2 Z_d Z_\alpha/r. \tag{6}$$

Before the separation the volume, surface and Coulomb energies are respectively given by:

$$E_V = -15.494(1 - 1.8I^2)A\ MeV, \tag{7}$$

$$E_S = 17.9439(1 - 2.6I^2)A^{2/3}(S/4\pi R_0^2)\ MeV, \tag{8}$$

$$E_C = 0.6e^2(Z^2/R_0) \times 0.5 \int (V(\theta)/V_0)(R(\theta)/R_0)^3 \sin\theta d\theta, \tag{9}$$

where I is the relative neutron excess, S the deformed surface, $V(\theta)$ the electrostatic potential at the surface and V_0 the surface potential of the sphere. The small energy gap appearing at the separation point due mainly to the difference between A_d/Z_d and A_α/Z_α has been linearized from the contact point to the sphere.

All along the decay path, the effects of the nucleon-nucleon force inside the neck or the gap between the nascent or separated α particle and daughter nucleus have been taken into account in a proximity energy term

$$E_{prox}(r) = 2\gamma \int_{h_{min}}^{h_{max}} \Phi[D(r,h)/b] 2\pi h dh, \tag{10}$$

where h is the ring radius in the plane perpendicular to the longitudinal deformation axis and D the distance between the opposite infinitesimal surfaces [13]. After the separation $h_{min} = 0$ and $h_{max} = R_\alpha$. b is the surface width fixed at the standard value of 0.99 fm. Φ is the universal proximity function [22]. The surface parameter γ is given by:

$$\gamma = 0.9517\sqrt{(1 - 2.6I_d^2)}\ MeV \cdot fm^{-2}. \tag{11}$$

In this GLDM the surface diffuseness is not considered in the surface energy term and the proximity energy vanishes when there is no neck as for spheres or ellipsoids for example.

The validity of this prescription to determine the proximity energy has been confirmed by the ability to reproduce accurately the fusion data [13,14]. Another test for the current macroscopic models is their efficiency to reproduce the asymmetric fission barrier heights of intermediate mass nuclei [23]. These new available data are extracted from excitation functions measured in heavy-ion reactions. In Fig. 1 shell corrected experimental barriers obtained recently [24] for ^{94,98}Mo are compared with the predictions of the Rotating Finite-Range Model [25], the Rotating Liquid Drop Model [26] and of our GLDM. The extracted barriers are several MeV higher on average than the calculated barriers by the Rotating Finite-Range Model and substantially lower than predicted by the Rotating Liquid Drop Model. The values given by the GLDM are in correct agreement with the experimental data. This supports the definition of the deformation energy in the GLDM and the parameter set which has never been changed since the first fission and fusion studies [13,15]. This validates also the hypothesis of a saddle-point corresponding to two separated nuclei maintained in unstable equilibrium by the balance between the repulsive Coulomb forces and the attractive proximity forces.

3 Potential barriers and α decay half-lives

As for the cluster emission [11], the experimental α decay Q value which incorporates the microscopic corrections plays a main role. It has been taken into account empirically in adding the difference between the experimental Q_α and the theoretical Q_α deduced from the GLDM at the macroscopic potential energy of the mother nucleus with a linear attenuation factor vanishing at the contact point of the nascent fragments.

The resulting potential barriers for the α decay of ^{108}Te and ^{264}Hs are displayed in Figs. 2 and 3. The maximum of the pure Coulomb barrier corresponds to the touching point between the nascent fragments. The introduction of the proximity forces lowers the barriers of 5.7 MeV for ^{108}Te and 7.3 MeV for ^{264}Hs. Furthermore the peak is shifted towards a more external position. The displacement is of 2.4 fm for ^{108}Te and 2.1 fm for ^{264}Hs. As a result, the approaches using the pure Coulomb barrier to determine the α decay barriers or the fusion barrier heights of the heaviest systems leading possibly to super heavy elements seem very rough. For example, for the $^{208}Pb + {}^{86}Kr$ reaction, the external fusion barrier height is lowered of 46 MeV when the proximity energy is taken into account.

In an unified fission model, the decay constant of the α emitter is simply defined as

$$\lambda = \nu_0 P, \tag{12}$$

without adjustable preformation factor. The assault frequency ν_0 has been taken as

$$\nu_0 = 10^{20}\ s^{-1}. \tag{13}$$

The barrier penetrability P is calculated within the action integral

$$P = exp[-\frac{2}{\hbar}\int_{R_{in}}^{R_{out}}\sqrt{2B(r)(E(r) - E(sphere))}dr]. \tag{14}$$

The deformation energy (relatively to the sphere) is small or even negative till the rupture point between the fragments (see Figs 2 and 3). Consequently, the two following approximations have been used :

$$R_{in} = R_d + R_\alpha, B(r) = \mu. \tag{15}$$

R_{out} is simply $e^2 Z_d Z_\alpha / Q_\alpha$. The partial half-life is related to the decay constant λ by

$$T_{1/2} = \frac{ln2}{\lambda}. \tag{16}$$

In tables 1, 2, 3 and 4 the position and height of the α decay barriers are given for 373 α emitters and the experimental and theoretical values of $log_{10}[T_{1/2}(s)]$ are compared. The experimental Q_α and $T_{1/2}$ values have been taken in [27–30].

The difference between R_{barr} and $R_d + R_\alpha$ is always at least 2 fm. The α decay barrier height varies between 10 and 17.5 MeV. For the subset of the 131 even-even nuclei the rms deviation between the values of $log_{10}[T_{1/2}(s)]$ obtained with the GLDM and the experimental ones is only 0.35. The theoretical data are slightly higher than the experimental ones for the lighter nuclei and systematically lower for the heaviest systems. For the other nuclides, the neglect of the angular momentum transfer and of the small probability of α particle preformation in the mother nucleus leads to a systematic slight underestimation of the experimental data and a rather higher deviation. Nevertheless, for the subsets of 106 even-odd, 86 odd-even and 50 odd-odd nuclei the rms deviations between the theoretical predictions and the experimental ones are respectively 0.71, 0.57 and 0.99. For the whole set of 373 α emitters the rms deviation is only 0.63.

Therefore, a correct evaluation of the α decay half-life is possible (at least for even-even nuclides) within a GLDM where the only input data are the mass A

and the charge Z of the α emitter and the experimental Q_α. There is no need to introduce variation of the assault frequency and systematic cluster preformation probability. This points out the basic importance of the proximity energy and the main role played by the experimental Q_α.

4 Analytical formulas for the α decay half-lives

The earliest law for the α decay half-lives was formulated by Geiger and Nutall [17]. Different expressions have been advanced later on [18–21]. A fitting procedure applied on the same set of 373 α emitters leads to the following formula with a rms deviation of 0.42.

$$\log_{10}[T_{1/2}(s)] = -26.06 - 1.114A^{1/6}\sqrt{Z} + \frac{1.5837\ Z}{\sqrt{Q_\alpha}}. \tag{17}$$

Assuming the same dependence on the mass and charge of the mother nucleus and experimental Q_α and adjusting to the subset of the 131 even-even nuclei, the relation (18) is obtained with a rms deviation of only 0.285.

$$\log_{10}[T_{1/2}(s)] = -25.31 - 1.1629A^{1/6}\sqrt{Z} + \frac{1.5864\ Z}{\sqrt{Q_\alpha}}. \tag{18}$$

For the subset of the 106 even-odd nuclei the rms deviation is 0.39 with the following formula.

$$\log_{10}[T_{1/2}(s)] = -26.65 - 1.0859A^{1/6}\sqrt{Z} + \frac{1.5848\ Z}{\sqrt{Q_\alpha}}. \tag{19}$$

The relation (20) corresponds to the subset of the 86 odd-even nuclei and a rms deviation of 0.36.

$$\log_{10}[T_{1/2}(s)] = -25.68 - 1.1423A^{1/6}\sqrt{Z} + \frac{1.592\ Z}{\sqrt{Q_\alpha}}. \tag{20}$$

Finally, for the subset of the 50 odd-odd nuclei the following formula leads to a rms of 0.35.

$$\log_{10}[T_{1/2}(s)] = -29.48 - 1.113A^{1/6}\sqrt{Z} + \frac{1.6971\ Z}{\sqrt{Q_\alpha}}. \tag{21}$$

5 Alpha decay half-lives of very heavy and super heavy elements

α decay half-lives of very heavy and super heavy elements deduced from the GLDM and from the fitted formulas (18-21) are presented in table V. When the experimental or simply extrapolated [27] Q_α is not available, the Thomas-Fermi model [31] has been used since it reproduces fairly well the experimental mass decrements of nuclei from fermium to elements $Z = 112$ [2]. For the even-even nuclei, the difference between the two values proposed for $log_{10}[T_{1/2}(s)]$ varies from 0.4 to 0.7. For all nuclei, the calculations within the GLDM should give a lower limit of the true value while the extrapolations from the formulas (18-21) should not be far from the reality provided Q_α is enough precise.

Recently, the $^{208}Pb + {}^{86}Kr$ and $^{244}Pu + {}^{48}Ca$ collisions around the Coulomb barrier energy have been studied at Berkeley [3] and Dubna [4]. The α decay chains of $^{293}118$ and $^{289}114$ have been observed. The way to analyse the experimental data is debated [5] and incomplete fusion cannot be exclude apparently. The measured ranges for $log_{10}[T_{1/2}(s)]$ are $^{293}118$ [-4.2, -3.5],$^{289}116$ [-3.5, -2.8], $^{285}114$ [-3.5, -2.8],$^{281}112$ [-3.4, -2.7],$^{277}110$ [-2.8, -2.1],^{273}Hs [-0.2, 0.5] and $^{289}114$ [0.3, 1.4], $^{285}112$ [3.1, 4.1] and $^{281}110$ [1.8, 2.9].

The data agree with our predictions except for $^{281}112$ and especially for $^{285}114$ and $^{289}114$ where the theoretical values are respectively of 5 and 2 orders of magnitude higher than the experimental data. The explanation of this discrepancy is perhaps that $Z = 114$ is not a magic number and that the Thomas-Fermi model underestimates Q_α for $Z = 114$ and then overestimates the half-lives. The experimental data must also perhaps be reanalyzed. It has been underlined [5] for the α-decay chain of $^{289}114$ that the deduced value of 190 MeV for the kinetic energy of the fission fragments at the end of the chain is two low. Within our fission model we obtain also a much higher value of 240 MeV. This is independent of the magicity of $Z = 114$. The memory of the entrance channel is perhaps also more important than generally considered. Further experiments are strongly needed and of major importance.

6 Summary and conclusion

The deformation energy of a nucleus emitting an α particle has been calculated within a GLDM including the proximity energy due to the attractive forces in the neck and the gap between the nascent α particle and daughter nucleus. The potential barrier is much lower than the pure Coulomb barrier and the top corresponds to fragments separated by more than 2 fm. After adjustment of the barrier to reproduce the experimental Q_α, the α decay half-lives have been calculated within the WKB barrier penetration probability and without

preformation factor which implicitly supposes that the α decay is rather a very asymmetric fission process.

For 373 α emitters, the rms deviation between the theoretical and the experimental values of $log_{10}[T_{1/2}(s)]$ is 0.63. For the even-even nuclei, the rms deviation is only 0.35. From theoretical Q_α, the α decay half-lives of the heaviest and super heavy systems have been calculated.

In addition, a fitting of the experimental data has led to analytic formulas for $log_{10}[T_{1/2}(s)]$. For the even-even nuclei, the rms deviation is 0.285. Extrapolations to very heavy and superheavy elements are proposed. The theoretical values are respectively of 5 and 2 orders of magnitude higher than the experimental data for the $^{285}114$ and the $^{289}114$ nuclei apparently observed recently. This might perhaps indicate that 114 is not a good magic proton number or that the data analysis must be pursued.

Acknowledgement

I thank G. Legoux, F. Roy, Y. Royer, B. Viaud and K. Zbiri who determined several tables and analytic fits.

References

[1] P. Armbruster, Ann. Rev. Nucl. Part. Sci 35 (1985) 135.

[2] S. Hofmann, preprint GSI 98-16 (1998).

[3] V. Ninov et al, Phys. Rev. Lett. 83 (1999) 1104.

[4] Y.T. Oganessian et al, Phys. Rev. Lett. 83 (1999) 3154.

[5] P. Armbruster, Preprint GSI 99-36 (1999), to be published in E. Phys. J. A.

[6] A.N. Andreyev et al, Z. Phys. A 358 (1997) 63.

[7] R.K. Gupta and W. Greiner, Int. J. Mod. Phys. E 3 (1994) 335.

[8] G. Gamow, Z. Phys. 51 (1928) 204.

[9] E.U. Condon and R.W. Gurney, Nature 122 (1928) 439.

[10] D.N. Poenaru, M. Ivascu, A. Sandulescu and W. Greiner, Phys. Rev. C 32 (1985) 572.

[11] G. Royer, R.K. Gupta and V.Y. Denisov, Nucl. Phys. A 632 (1998) 275.

[12] S. Kumar, R.K. Gupta and W. Scheid, Int. J. Mod. Phys. E 3 (1994) 195.

[13] G. Royer and B. Remaud, Nucl. Phys. A 444 (1985) 477.

[14] G. Royer, C. Normand and E. Druet, Nucl. Phys. A 634 (1998) 267.

[15] G. Royer and B. Remaud, J. Phys. G 10 (1984) 1057.

[16] G. Royer, in Heavy Elements and Related New Phenomena, ed. R.K. Gupta and W. Greiner (World Scientific, 1999) p.591.

[17] H. Geiger and J.M. Nutall, Philos. Mag. 22 (1911) 613.

[18] V.E. Viola and G.T. Seaborg, J. Inorg. Nucl. Chem. 28 (1966) 741.

[19] D.N. Poenaru and M. Ivascu, J. Phys. (Paris) 44 (1983) 791.

[20] B.A. Brown, Phys. Rev. C 46 (1992) 811.

[21] D.N. Poenaru and W. Greiner, Nuclear Decay Modes, (Institute of Physics Publishing, Bristol, 1996) p.224.

[22] H. Feldmeier, 12th Summer School on nuclear physics, Mikolajki, Poland, 1979.

[23] G. Royer and F. Haddad, Phys. Rev. C 51 (1995) 2813.

[24] K.X. Jing et al, Nucl. Phys. A 645 (1999) 203.

[25] A.J. Sierk, Phys. Rev. Lett. 55 (1985) 582.

[26] A.J. Sierk, Phys. Rev. C 33 (1986) 2039.

[27] G. Audi, O. Bersillon, J. Blachot and A.H. Wapstra, Nucl. Phys. A 624 (1997) 1.

[28] D.N. Poenaru and M. Ivascu, Rev. Roum. Phys 28 (1983) 309.

[29] R.B. Firestone, Table of isotopes (J Wiley & Sons, New York, 1996).

[30] O.A.P Tavares, S.B. Duarte, O. Rodriguez, F. Guzman, M. Goncalves and F. Garcia, J. Phys. G 24 (1998) 1757.

[31] W.D. Myers and W.J. Swiatecki, preprint LBL-36803 (1994) and Nucl. Phys. A 601 (1996) 141.

Table captions

Table 1. Characteristics of α decay for 131 even-even nuclei. The first column indicates the mother nucleus. The second one gives the distance between the mass centres of the α particle and the daughter nucleus at the contact point. The third and fourth columns correspond respectively to the distance between the mass centres and height at the top of the potential barrier. The experimental Q_α is given in the fifth column. The experimental value of $log_{10}[T_{1/2}(s)]$ and the theoretical value obtained with the GLDM are compared in the two last columns.

Table 2. Same as table 1 but for 106 even-odd nuclei.

Table 3. Same as table 1 but for 86 odd-even nuclei.

Table 4. Same as table 1 but for 50 odd-odd nuclei.

Table 5. $log_{10}[T_{1/2}(s)]$ for the heaviest and super heavy elements as functions of the charge and mass of the mother nucleus and Q_α. The symbol # corresponds to the Thomas-Fermi model predictions [31] for Q_α. The absence of symbol means that Q_α is extracted from [27,28]. The third and fourth lines give respectively the values of $log_{10}[T_{1/2}(s)]$ obtained by the GLDM and the values extrapolated from the four fitted formulas (18-21).

Figure captions

Fig. 1. Comparison of the shell corrected experimental fission barrier heights B_Z with the macroscopic barrier heights given by the Rotating Finite-Range Model, the Rotating Liquid Drop Model and our GLDM for ^{94,98}Mo.

Fig. 2. α decay barrier including empirical microscopic corrections of the ^{108}Te mother nucleus. The dashed and solid curves correspond respectively to the deformation energy without and with a nuclear proximity energy term. r is the centre-of-mass distance.

Fig. 3. Same as Fig. 2. but for the ^{264}Hs mother nucleus.

Table 1

nuclide	R_d+R_α (fm)	R_{barr} (fm)	E_{barr} (MeV)	Q_{exp} (MeV)	$\log_{10}$ ($T_{1/2\ exp}$)	$\log_{10}$ ($T_{1/2\ theo}$)
$^{108}_{52}Te$	7.2	9.6	10.5	3.44	0.63	1.02
$^{110}_{52}Te$	7.3	9.65	11.15	2.72	5.79	6.54
$^{110}_{54}Xe$	7.3	9.55	10.6	3.88	-0.4	-0.35
$^{112}_{54}Xe$	7.3	9.6	11.1	3.32	2.51	3.14
$^{144}_{60}Nd$	7.8	10.1	13.4	1.90	22.82	23.62
$^{146}_{62}Sm$	7.9	10.2	13.3	2.53	15.51	15.86
$^{148}_{62}Sm$	7.9	10.2	13.8	1.99	23.4	23.90
$^{148}_{64}Gd$	7.9	10.2	13.05	3.27	9.36	9.68
$^{150}_{64}Gd$	7.9	10.3	13.5	2.81	13.75	14.09
$^{152}_{64}Gd$	7.95	10.2	14.0	2.20	21.54	22.12
$^{150}_{66}Dy$	7.9	10.15	12.5	4.35	3.13	3.22
$^{152}_{66}Dy$	7.95	10.2	13.0	3.73	6.93	7.25
$^{154}_{66}Dy$	8.0	10.2	13.8	2.95	13.98	14.07
$^{152}_{68}Er$	7.95	10.2	12.4	4.93	1.04	1.21
$^{154}_{68}Er$	8.0	10.2	13.0	4.28	4.69	4.76
$^{154}_{70}Yb$	8.0	10.2	12.4	5.47	-0.4	-0.29
$^{156}_{70}Yb$	8.0	10.3	13.0	4.81	2.41	2.80
$^{156}_{72}Hf$	8.0	10.3	12.3	6.03	-1.6	-1.67
$^{158}_{72}Hf$	8.0	10.3	12.9	5.40	0.84	0.93
$^{162}_{72}Hf$	8.1	10.4	13.75	4.42	5.69	6.08
$^{162}_{74}W$	8.1	10.3	13.05	5.67	0.48	0.66
$^{164}_{74}W$	8.1	10.3	13.4	5.28	2.39	2.38
$^{166}_{74}W$	8.15	10.35	13.8	4.86	4.67	4.52
$^{166}_{76}Os$	8.15	10.35	13.0	6.13	-0.52	-0.40
$^{168}_{76}Os$	8.2	10.4	13.3	5.82	0.65	0.85
$^{170}_{76}Os$	8.2	10.4	13.5	5.54	1.79	2.02
$^{172}_{76}Os$	8.2	10.5	13.8	5.23	3.98	3.50
$^{174}_{76}Os$	8.3	10.5	14.1	4.87	5.35	5.40
$^{186}_{76}Os$	8.4	10.6	15.9	2.82	22.8	22.66
$^{172}_{78}Pt$	8.2	10.5	13.1	6.46	-0.96	-0.90
$^{174}_{78}Pt$	8.3	10.5	13.3	6.18	0.04	0.16
$^{176}_{78}Pt$	8.3	10.5	13.6	5.89	1.18	1.34
$^{178}_{78}Pt$	8.3	10.6	13.8	5.57	2.47	2.71
$^{180}_{78}Pt$	8.3	10.6	14.1	5.26	4.22	4.22
$^{182}_{78}Pt$	8.4	10.6	14.4	4.94	5.89	5.93
$^{184}_{78}Pt$	8.4	10.55	14.7	4.59	8.02	8.02
$^{186}_{78}Pt$	8.4	10.6	14.9	4.32	9.71	9.74
$^{188}_{78}Pt$	8.45	10.6	15.15	4.01	12.47	12.02
$^{190}_{78}Pt$	8.5	10.7	15.9	3.25	19.34	19.01

$^{176}_{80}Hg$	8.3	10.5	13.1	6.92	-1.7	-1.76
$^{178}_{80}Hg$	8.3	10.6	13.35	6.58	-0.44	-0.60
$^{182}_{80}Hg$	8.4	10.5	13.8	6.00	1.85	1.68
$^{184}_{80}Hg$	8.4	10.6	14.1	5.66	3.37	3.20
$^{186}_{80}Hg$	8.4	10.6	14.5	5.21	5.73	5.40
$^{182}_{82}Pb$	8.4	10.5	13.3	7.08	-1.26	-1.59
$^{210}_{82}Pb$	8.7	10.9	15.9	3.79	16.57	16.00
$^{194}_{84}Po$	8.5	10.7	13.6	6.99	-0.41	-0.69
$^{196}_{84}Po$	8.55	10.8	13.9	6.66	0.76	0.51
$^{198}_{84}Po$	8.6	10.8	14.2	6.31	2.18	1.91
$^{200}_{84}Po$	8.6	10.8	14.5	5.98	3.79	3.28
$^{202}_{84}Po$	8.6	10.9	14.7	5.70	5.13	4.59
$^{204}_{84}Po$	8.65	10.9	14.9	5.48	6.28	5.69
$^{206}_{84}Po$	8.7	10.9	15.0	5.33	7.15	6.47
$^{208}_{84}Po$	8.7	10.8	15.1	5.22	7.97	7.07
$^{212}_{84}Po$	8.75	10.9	11.25	8.95	-6.52	-6.84
$^{214}_{84}Po$	8.8	10.9	12.3	7.83	-3.78	-3.82
$^{216}_{84}Po$	8.8	10.95	13.2	6.90	-0.82	-0.74
$^{218}_{84}Po$	8.8	11.0	14.0	6.11	2.27	2.37
$^{200}_{86}Rn$	8.6	10.8	13.9	7.04	0.0	-0.15
$^{202}_{86}Rn$	8.6	10.9	14.1	6.77	1.06	0.84
$^{204}_{86}Rn$	8.65	10.8	14.3	6.55	2.00	1.69
$^{206}_{86}Rn$	8.7	10.8	14.5	6.38	2.71	2.37
$^{208}_{86}Rn$	8.7	10.8	14.5	6.26	3.34	2.86
$^{210}_{86}Rn$	8.7	10.9	14.6	6.16	3.96	3.23
$^{212}_{86}Rn$	8.75	10.9	14.3	6.38	3.17	2.25
$^{214}_{86}Rn$	8.8	10.9	11.5	9.21	-6.57	-6.82
$^{216}_{86}Rn$	8.8	10.95	12.4	8.20	-4.35	-4.21
$^{218}_{86}Rn$	8.8	11.0	13.3	7.26	-1.45	-1.26
$^{220}_{86}Rn$	8.8	11.0	14.1	6.40	1.75	2.02
$^{222}_{86}Rn$	8.9	11.0	14.9	5.59	5.52	5.80
$^{206}_{88}Ra$	8.7	10.8	13.9	7.42	-0.62	-0.75
$^{208}_{88}Ra$	8.7	10.8	14.0	7.27	0.15	-0.26
$^{210}_{88}Ra$	8.7	10.9	14.1	7.16	0.56	0.07
$^{212}_{88}Ra$	8.75	10.9	14.2	7.03	1.15	0.53
$^{214}_{88}Ra$	8.8	10.9	13.9	7.27	0.4	-0.38
$^{216}_{88}Ra$	8.8	10.95	11.6	9.53	-6.74	-6.93
$^{218}_{88}Ra$	8.8	11.0	12.5	8.55	-4.59	-4.49
$^{220}_{88}Ra$	8.8	11.0	13.45	7.60	-1.74	-1.63
$^{222}_{88}Ra$	8.9	11.0	14.3	6.68	1.59	1.72
$^{224}_{88}Ra$	8.9	11.1	15.2	5.79	5.53	5.74
$^{226}_{88}Ra$	8.9	11.1	16.1	4.87	10.73	10.98
$^{214}_{90}Th$	8.8	10.9	13.9	7.83	-1.0	-1.48
$^{216}_{90}Th$	8.8	10.95	13.6	8.07	-1.55	-2.28

$^{220}_{90}Th$	8.8	11.0	12.6	8.95	-5.01	-4.89
$^{222}_{90}Th$	8.9	11.0	13.4	8.13	-2.55	-2.58
$^{224}_{90}Th$	8.9	11.1	14.2	7.30	0.11	0.17
$^{226}_{90}Th$	8.9	11.1	15.0	6.45	3.39	3.49
$^{228}_{90}Th$	8.9	11.1	15.9	5.52	7.92	8.07
$^{230}_{90}Th$	8.95	11.2	16.6	4.77	12.51	12.75
$^{232}_{90}Th$	9.0	11.2	17.2	4.08	17.76	18.18
$^{228}_{92}U$	8.9	11.1	15.1	6.80	2.76	2.86
$^{230}_{92}U$	8.95	11.2	15.9	5.99	6.43	6.54
$^{232}_{92}U$	9.0	11.2	16.4	5.41	9.52	9.69
$^{234}_{92}U$	9.0	11.1	16.9	4.86	13.02	13.21
$^{236}_{92}U$	9.0	11.1	17.15	4.57	14.99	15.23
$^{238}_{92}U$	9.0	11.15	17.41	4.27	17.27	17.63
$^{232}_{94}Pu$	9.0	11.1	15.6	6.72	4.20	4.04
$^{234}_{94}Pu$	9.0	11.1	15.95	6.31	5.72	5.88
$^{236}_{94}Pu$	9.0	11.1	16.35	5.87	8.1	8.01
$^{238}_{94}Pu$	9.0	11.15	16.6	5.59	9.59	9.54
$^{240}_{94}Pu$	9.1	11.2	16.9	5.26	11.45	11.51
$^{242}_{94}Pu$	9.1	11.2	17.1	4.98	13.19	13.34
$^{244}_{94}Pu$	9.1	11.2	17.4	4.66	15.51	15.55
$^{240}_{96}Cm$	9.1	11.2	16.2	6.40	6.52	6.25
$^{242}_{96}Cm$	9.1	11.2	16.4	6.22	7.28	7.11
$^{244}_{96}Cm$	9.1	11.2	16.7	5.90	8.87	8.68
$^{246}_{96}Cm$	9.1	11.3	17.0	5.47	11.28	11.12
$^{248}_{96}Cm$	9.15	11.3	17.3	5.16	13.15	13.08
$^{250}_{96}Cm$	9.2	11.3	17.3	5.17	12.45	12.99
$^{240}_{98}Cf$	9.1	11.2	15.4	7.72	1.8	1.62
$^{242}_{98}Cf$	9.1	11.2	15.6	7.52	2.44	2.33
$^{244}_{98}Cf$	9.1	11.2	15.7	7.33	3.18	2.99
$^{246}_{98}Cf$	9.1	11.3	16.1	6.86	5.22	4.92
$^{248}_{98}Cf$	9.1	11.3	16.6	6.36	7.46	7.23
$^{250}_{98}Cf$	9.2	11.3	16.8	6.13	8.69	8.37
$^{252}_{98}Cf$	9.2	11.3	16.7	6.22	8.0	7.88
$^{254}_{98}Cf$	9.2	11.4	16.9	5.93	9.31	9.33
$^{246}_{100}Fm$	9.1	11.3	15.1	8.37	0.12	0.03
$^{248}_{100}Fm$	9.1	11.3	15.5	8.00	1.67	1.27
$^{250}_{100}Fm$	9.2	11.3	15.9	7.56	3.25	2.86
$^{252}_{100}Fm$	9.2	11.3	16.2	7.15	4.98	4.48
$^{254}_{100}Fm$	9.2	11.4	16.0	7.31	4.14	3.75
$^{256}_{100}Fm$	9.2	11.4	16.3	7.03	5.11	4.89
$^{252}_{102}No$	9.2	11.3	15.3	8.55	0.62	0.11

$^{254}_{102}No$	9.2	11.4	15.6	8.23	1.86	1.12
$^{256}_{102}No$	9.2	11.4	15.2	8.58	0.54	-0.07
$^{256}_{104}Rf$	9.2	11.4	15.3	8.95	-0.44	-0.51
$^{260}_{106}Sg$	9.3	11.3	14.8	9.93	-2.07	-2.70
$^{266}_{106}Sg$	9.3	11.4	15.8	8.76	1.53	0.66
$^{264}_{108}Hs$	9.3	11.4	14.5	10.58	-3.6	-3.81

Table 2

nuclide	R_d+R_α (fm)	R_{barr} (fm)	E_{barr} (MeV)	Q_{exp} (MeV)	$\log_{10}$ ($T_{1/2\ exp}$)	$\log_{10}$ ($T_{1/2\ theo}$)
$^{107}_{52}Te$	7.2	9.6	9.96	4.0	-2.29	-2.17
$^{109}_{52}Te$	7.2	9.6	10.7	3.23	2.01	2.42
$^{111}_{54}Xe$	7.3	9.6	10.7	3.71	-0.05	0.62
$^{113}_{54}Xe$	7.3	9.6	11.3	3.10	3.9	4.70
$^{147}_{62}Sm$	7.9	10.2	13.5	2.31	18.54	18.79
$^{149}_{64}Gd$	7.9	10.2	13.2	3.10	11.21	11.15
$^{151}_{64}Gd$	7.9	10.3	13.6	2.65	15.11	15.92
$^{151}_{66}Dy$	7.9	10.2	12.6	4.18	4.26	4.23
$^{153}_{66}Dy$	8.0	10.2	13.2	3.56	8.9	8.53
$^{153}_{68}Er$	8.0	10.2	12.5	4.80	1.85	1.85
$^{155}_{68}Er$	8.0	10.2	13.1	4.12	6.16	5.76
$^{155}_{70}Yb$	8.0	10.25	12.5	5.34	0.25	0.27
$^{157}_{70}Yb$	8.0	10.3	13.1	4.62	3.89	3.82
$^{157}_{72}Hf$	8.0	10.3	12.4	5.88	-0.92	-1.10
$^{159}_{72}Hf$	8.05	10.3	13.0	5.22	1.15	1.75
$^{161}_{72}Hf$	8.1	10.4	13.5	4.71	3.76	4.38
$^{163}_{74}W$	8.1	10.3	13.2	5.52	0.83	1.27
$^{167}_{76}Os$	8.2	10.4	13.2	5.98	0.08	0.19
$^{169}_{76}Os$	8.2	10.4	13.4	5.72	1.49	1.27
$^{171}_{76}Os$	8.2	10.4	13.7	5.37	2.68	2.81
$^{173}_{76}Os$	8.25	10.5	13.9	5.06	4.88	4.37
$^{173}_{78}Pt$	8.25	10.5	13.2	6.35	-0.39	-0.50
$^{175}_{78}Pt$	8.3	10.5	13.3	6.18	0.53	0.14
$^{177}_{78}Pt$	8.3	10.55	13.8	5.64	2.30	2.40
$^{179}_{78}Pt$	8.3	10.6	14.1	5.28	4.09	4.13
$^{181}_{78}Pt$	8.4	10.6	14.2	5.13	4.93	4.90
$^{183}_{78}Pt$	8.4	10.5	14.4	4.84	7.48	6.50
$^{177}_{80}Hg$	8.3	10.55	13.2	6.74	-0.77	-1.17
$^{179}_{80}Hg$	8.3	10.5	13.5	6.43	0.32	-0.04
$^{181}_{80}Hg$	8.4	10.5	13.6	6.29	1.32	0.49
$^{183}_{80}Hg$	8.4	10.5	13.8	6.04	1.57	1.50
$^{189}_{82}Pb$	8.5	10.6	14.4	5.85	4.11	3.17
$^{191}_{82}Pb$	8.5	10.7	14.7	5.41	5.78	5.31
$^{193}_{84}Po$	8.5	10.7	13.5	7.1	-0.59	-1.07
$^{195}_{84}Po$	8.5	10.7	13.8	6.75	0.79	0.18
$^{197}_{84}Po$	8.6	10.8	14.1	6.41	2.08	1.50
$^{199}_{84}Po$	8.6	10.8	14.4	6.07	3.64	2.94
$^{201}_{84}Po$	8.6	10.8	14.6	5.80	4.76	4.11

$^{203}_{84}Po$	8.6	10.9	14.9	5.50	6.31	5.59
$^{205}_{84}Po$	8.7	10.9	15.0	5.32	7.18	6.54
$^{207}_{84}Po$	8.7	10.8	15.1	5.22	8.00	7.08
$^{209}_{84}Po$	8.7	10.8	15.3	4.98	9.51	8.40
$^{213}_{84}Po$	8.8	10.9	11.6	8.54	-5.37	-5.81
$^{215}_{84}Po$	8.8	10.9	12.6	7.53	-2.74	-2.89
$^{217}_{84}Po$	8.8	11.0	13.4	6.66	1.0	0.10
$^{201}_{86}Rn$	8.6	10.8	14.1	6.86	0.85	0.50
$^{203}_{86}Rn$	8.6	10.9	14.3	6.63	1.83	1.37
$^{205}_{86}Rn$	8.7	10.8	14.5	6.39	2.86	2.34
$^{207}_{86}Rn$	8.7	10.8	14.6	6.25	3.39	2.93
$^{209}_{86}Rn$	8.7	10.8	14.6	6.15	4.0	3.28
$^{211}_{86}Rn$	8.7	10.9	14.8	5.89	5.5	4.47
$^{215}_{86}Rn$	8.8	10.9	11.8	8.84	-5.64	-5.92
$^{217}_{86}Rn$	8.8	11.0	12.7	7.89	-3.26	-3.30
$^{219}_{86}Rn$	8.8	11.0	13.6	6.95	0.69	-0.16
$^{221}_{86}Rn$	8.85	11.0	14.4	6.15	3.92	3.10
$^{207}_{88}Ra$	8.7	10.8	14.1	7.27	0.11	-0.23
$^{209}_{88}Ra$	8.7	10.8	14.1	7.15	0.66	0.12
$^{211}_{88}Ra$	8.7	10.9	14.2	7.05	1.08	0.46
$^{213}_{88}Ra$	8.8	10.9	14.45	6.75	2.62	1.60
$^{217}_{88}Ra$	8.8	11.0	11.95	9.16	-5.8	-6.08
$^{221}_{88}Ra$	8.85	11.0	14.3	6.73	1.92	1.53
$^{223}_{88}Ra$	8.9	11.1	15.1	5.87	6.27	5.35
$^{213}_{90}Th$	8.8	10.9	13.9	7.84	-0.82	-1.49
$^{215}_{90}Th$	8.8	10.9	14.1	7.54	0.36	-0.52
$^{219}_{90}Th$	8.8	11.0	12.1	9.51	-6.0	-6.29
$^{221}_{90}Th$	8.85	11.0	13.2	8.30	-2.54	-3.08
$^{223}_{90}Th$	8.9	11.1	14.1	7.42	0.04	-0.25
$^{225}_{90}Th$	8.9	11.1	14.9	6.59	3.07	2.95
$^{229}_{90}Th$	8.9	11.15	16.4	4.93	11.61	11.66
$^{227}_{92}U$	8.9	11.1	14.9	7.21	1.82	2.95
$^{229}_{92}U$	8.9	11.1	15.4	6.47	4.34	4.27
$^{231}_{92}U$	9.0	11.2	16.3	5.55	9.82	8.89
$^{233}_{92}U$	9.0	11.2	16.9	4.91	12.78	12.87
$^{235}_{92}U$	9.0	11.1	17.3	4.48	16.57	15.94
$^{233}_{94}Pu$	9.0	11.1	15.9	6.42	6.02	5.38

$^{235}_{94}Pu$	9.0	11.1	16.2	6.00	7.7	7.34
$^{237}_{94}Pu$	9.0	11.1	16.75	5.45	11.17	10.37
$^{239}_{94}Pu$	9.1	11.2	16.9	5.24	12.01	11.65
$^{241}_{94}Pu$	9.1	11.2	17.1	4.98	13.34	13.35
$^{239}_{96}Cm$	9.1	11.2	16.2	6.5	7.03	5.79
$^{241}_{96}Cm$	9.1	11.2	16.6	6.04	8.61	8.04
$^{243}_{96}Cm$	9.1	11.2	16.7	5.88	9.08	8.87
$^{245}_{96}Cm$	9.1	11.25	17.1	5.45	11.46	11.25
$^{247}_{96}Cm$	9.1	11.3	17.1	4.95	14.85	14.54
$^{241}_{98}Cf$	9.1	11.2	15.5	7.66	3.36	1.83
$^{243}_{98}Cf$	9.1	11.2	15.8	7.28	3.79	3.26
$^{245}_{98}Cf$	9.1	11.25	15.8	7.26	3.94	3.26
$^{251}_{98}Cf$	9.2	11.3	17.1	5.77	10.91	10.32
$^{253}_{98}Cf$	9.2	11.4	16.75	6.12	8.72	8.32
$^{245}_{100}Fm$	9.1	11.25	15.1	8.44	0.62	-0.19
$^{247}_{100}Fm$	9.1	11.3	15.3	8.19	2.07	0.62
$^{249}_{100}Fm$	9.2	11.3	15.6	7.81	2.59	1.93
$^{251}_{100}Fm$	9.2	11.3	16.5	6.94	6.07	5.40
$^{253}_{100}Fm$	9.2	11.4	16.3	7.05	6.7	4.84
$^{255}_{100}Fm$	9.2	11.4	16.2	7.13	4.88	4.48
$^{257}_{100}Fm$	9.25	11.4	16.7	6.62	6.87	6.73
$^{251}_{102}No$	9.2	11.3	15.1	8.74	0.0	-0.48
$^{253}_{102}No$	9.2	11.4	15.4	8.44	2.02	0.42
$^{255}_{102}No$	9.2	11.4	15.6	8.25	2.81	1.04
$^{257}_{102}No$	9.2	11.4	15.3	8.45	2.14	0.34
$^{259}_{102}No$	9.3	11.4	15.8	7.62	4.06	3.29
$^{261}_{104}Rf$	9.3	11.5	15.4	8.60	1.86	0.55
$^{263}_{106}Sg$	9.3	11.35	14.9	9.39	-0.04	-1.24
$^{265}_{106}Sg$	9.3	11.4	15.8	8.76	0.85	0.67
$^{265}_{108}Hs$	9.3	11.4	14.6	10.47	-2.80	-3.55
$^{269}_{110}$	9.4	11.4	14.2	11.28	-3.77	-4.88

Table 3

nuclide	R_d+R_α (fm)	R_{barr} (fm)	E_{barr} (MeV)	Q_{exp} (MeV)	$\log_{10}$ ($T_{1/2\ exp}$)	$\log_{10}$ ($T_{1/2\ theo}$)
$^{111}_{53}I$	7.3	9.6	10.9	3.28	3.45	2.74
$^{145}_{61}Pm$	7.85	10.2	13.2	2.32	17.28	17.79
$^{147}_{63}Eu$	7.9	10.2	13.1	2.99	10.99	11.56
$^{149}_{65}Tb$	7.9	10.2	12.5	4.08	4.96	4.27
$^{151}_{65}Tb$	7.9	10.2	13.0	3.50	8.82	8.36
$^{151}_{67}Ho$	7.9	10.2	12.4	4.70	2.26	1.85
$^{153}_{67}Ho$	8.0	10.2	13.0	4.05	5.46	5.64
$^{153}_{69}Tm$	8.0	10.2	12.3	5.25	0.25	0.20
$^{155}_{69}Tm$	8.0	10.25	13.0	4.57	3.04	3.62
$^{155}_{71}Lu$	8.0	10.25	12.3	5.77	-1.05	-1.07
$^{157}_{71}Lu$	8.0	10.3	12.9	5.10	1.88	1.85
$^{157}_{73}Ta$	8.0	10.3	12.2	6.38	-2.28	-2.52
$^{159}_{73}Ta$	8.05	10.3	12.8	5.75	-0.15	-0.12
$^{161}_{73}Ta$	8.1	10.25	13.2	5.27	1.78	2.00
$^{169}_{77}Ir$	8.2	10.4	13.1	6.28	-0.4	-0.58
$^{171}_{77}Ir$	8.25	10.4	13.1	6.16	0.23	-0.18
$^{173}_{77}Ir$	8.25	10.5	13.1	5.84	0.48	1.12
$^{177}_{79}Au$	8.3	10.55	13.3	6.43	0.11	-0.46
$^{179}_{79}Au$	8.3	10.6	13.6	6.08	1.51	0.91
$^{181}_{79}Au$	8.4	10.5	13.8	5.75	3.28	2.33
$^{183}_{79}Au$	8.4	10.5	14.1	5.47	4.17	3.63
$^{185}_{79}Au$	8.4	10.6	14.3	5.18	4.99	5.04
$^{189}_{83}Bi$	8.5	10.6	13.2	6.81	0.18	-0.35
$^{191}_{83}Bi$	8.5	10.7	13.6	6.46	1.51	0.98
$^{193}_{83}Bi$	8.5	10.7	14.1	6.04	2.1	2.70
$^{195}_{83}Bi$	8.5	10.7	14.5	5.56	4.92	4.94
$^{197}_{85}At$	8.6	10.8	13.7	7.1	-0.4	-0.71
$^{199}_{85}At$	8.6	10.8	14.0	6.78	0.85	0.45
$^{201}_{85}At$	8.6	10.8	14.2	6.47	2.1	1.60
$^{203}_{85}At$	8.6	10.9	14.4	6.21	3.16	2.68
$^{205}_{85}At$	8.7	10.9	14.6	6.02	4.19	3.51
$^{207}_{85}At$	8.7	10.8	14.7	5.87	4.81	4.20
$^{209}_{85}At$	8.7	10.8	14.8	5.76	5.68	4.64
$^{211}_{85}At$	8.7	10.9	14.5	5.98	4.79	3.57
$^{213}_{85}At$	8.8	10.9	11.2	9.25	-6.96	-7.23
$^{215}_{85}At$	8.8	10.9	12.2	8.18	-4.0	-4.48
$^{217}_{85}At$	8.8	11.0	13.1	7.20	-1.48	-1.46
$^{219}_{85}At$	8.8	11.0	13.9	6.39	1.75	1.62
$^{203}_{87}Fr$	8.6	10.75	13.9	7.28	-0.15	-0.64
$^{205}_{87}Fr$	8.7	10.8	14.1	7.06	0.58	0.13
$^{207}_{87}Fr$	8.7	10.8	14.2	6.90	1.21	0.71

$^{209}_{87}Fr$	8.7	10.8	14.25	6.78	1.75	1.09
$^{211}_{87}Fr$	8.7	10.9	14.3	6.66	2.27	1.54
$^{213}_{87}Fr$	8.8	10.9	14.0	6.90	1.55	0.58
$^{215}_{87}Fr$	8.8	10.9	11.4	9.54	-7.06	-7.26
$^{217}_{87}Fr$	8.8	11.0	12.4	8.47	-4.79	-4.62
$^{219}_{87}Fr$	8.8	11.0	13.4	7.45	-1.67	-1.52
$^{221}_{87}Fr$	8.85	11.0	14.3	6.46	2.54	2.20
$^{223}_{87}Fr$	8.9	11.1	15.3	5.43	7.34	7.16
$^{209}_{89}Ac$	8.7	10.8	13.8	7.73	-1.0	-1.48
$^{211}_{89}Ac$	8.7	10.9	13.9	7.62	-0.6	-1.14
$^{213}_{89}Ac$	8.8	10.9	14.0	7.5	-0.1	-0.76
$^{215}_{89}Ac$	8.8	10.9	13.7	7.75	-0.77	-1.63
$^{217}_{89}Ac$	8.8	11.0	11.5	9.83	-7.16	-7.31
$^{219}_{89}Ac$	8.8	11.0	12.5	8.83	-4.92	-4.91
$^{221}_{89}Ac$	8.85	11.0	13.5	7.78	-1.13	-1.84
$^{223}_{89}Ac$	8.9	11.1	14.5	6.77	2.47	1.78
$^{225}_{89}Ac$	8.9	11.1	15.3	5.93	6.23	5.52
$^{227}_{89}Ac$	8.9	11.1	16.1	5.04	11.01	10.42
$^{213}_{91}Pa$	8.8	10.9	13.6	8.39	-2.28	-2.82
$^{215}_{91}Pa$	8.8	10.9	13.8	8.17	-1.85	-2.19
$^{217}_{91}Pa$	8.8	11.0	13.4	8.49	-2.46	-3.21
$^{223}_{91}Pa$	8.9	11.1	13.4	8.34	-1.84	-2.85
$^{225}_{91}Pa$	8.9	11.1	14.3	7.39	0.41	0.25
$^{227}_{91}Pa$	8.9	11.1	15.1	6.58	3.72	3.36
$^{229}_{91}Pa$	8.9	11.1	15.9	5.68	8.12	7.69
$^{229}_{93}Np$	8.9	11.15	15.1	7.01	2.38	2.43
$^{231}_{93}Np$	9.0	11.2	15.7	6.37	5.17	5.17
$^{233}_{93}Np$	9.0	11.1	16.2	5.83	8.34	7.83
$^{235}_{93}Np$	9.0	11.1	16.9	5.11	12.66	11.98
$^{237}_{93}Np$	9.0	11.1	17.1	4.87	14.16	13.59
$^{237}_{95}Am$	9.0	11.1	16.2	6.25	7.24	6.54
$^{239}_{95}Am$	9.1	11.2	16.5	5.87	8.72	8.47
$^{241}_{95}Am$	9.1	11.2	16.8	5.58	10.2	10.08
$^{243}_{95}Am$	9.1	11.2	17.0	5.36	11.43	11.38
$^{245}_{97}Bk$	9.1	11.25	16.8	5.99	9.21	8.67
$^{247}_{97}Bk$	9.1	11.3	17.1	5.62	10.99	10.73
$^{249}_{97}Bk$	9.2	11.3	17.2	5.51	12.41	11.37
$^{243}_{99}Es$	9.1	11.2	15.3	8.07	1.32	0.73
$^{245}_{99}Es$	9.1	11.25	15.4	7.91	2.66	1.22
$^{247}_{99}Es$	9.1	11.3	15.75	7.49	3.63	2.75
$^{249}_{99}Es$	9.2	11.3	16.3	6.94	5.83	4.98
$^{251}_{99}Es$	9.2	11.3	16.6	6.60	7.48	6.50
$^{253}_{99}Es$	9.2	11.4	16.4	6.74	6.29	5.76
$^{255}_{99}Es$	9.2	11.4	16.6	6.44	7.69	7.16
$^{259}_{103}Lr$	9.3	11.4	15.3	8.67	0.73	-0.03

Table 4

nuclide	R_d+R_α (fm)	R_{barr} (fm)	E_{barr} (MeV)	Q_{exp} (MeV)	$\log_{10}$ ($T_{1/2\ exp}$)	$\log_{10}$ ($T_{1/2\ theo}$)
$^{110}_{53}I$	7.3	9.55	10.6	3.58	0.58	0.77
$^{114}_{55}Cs$	7.3	9.65	11.3	3.36	3.5	3.46
$^{148}_{63}Eu$	7.9	10.2	13.3	2.76	14.7	13.95
$^{152}_{67}Ho$	7.95	10.2	12.5	4.51	3.11	2.86
$^{154}_{67}Ho$	8.0	10.2	13.0	4.04	6.63	5.69
$^{154}_{69}Tm$	8.0	10.2	12.5	5.09	1.05	0.93
$^{156}_{69}Tm$	8.0	10.3	13.2	4.34	5.15	4.90
$^{156}_{71}Lu$	8.0	10.3	12.5	5.59	-0.3	-0.37
$^{158}_{73}Ta$	8.0	10.3	12.3	6.21	-1.4	-1.92
$^{170}_{77}Ir$	8.2	10.4	13.2	6.17	0.15	-0.20
$^{172}_{77}Ir$	8.2	10.5	13.3	5.99	0.23	0.50
$^{178}_{79}Au$	8.3	10.6	13.5	6.12	0.42	0.76
$^{184}_{79}Au$	8.4	10.55	14.2	5.3	5.38	4.48
$^{192}_{83}Bi$	8.5	10.7	14.0	6.19	2.32	2.035
$^{194}_{83}Bi$	8.5	10.7	14.4	5.76	4.72	3.97
$^{196}_{85}At$	8.6	10.8	13.6	7.2	-0.52	-1.05
$^{198}_{85}At$	8.6	10.8	13.9	6.89	0.69	0.05
$^{200}_{85}At$	8.6	10.8	14.1	6.60	1.33	1.09
$^{202}_{85}At$	8.6	10.9	14.4	6.26	3.38	2.48
$^{204}_{85}At$	8.65	10.9	14.6	6.07	4.07	3.29
$^{206}_{85}At$	8.7	10.8	14.9	5.72	5.29	4.94
$^{208}_{85}At$	8.7	10.8	14.8	5.75	6.03	4.77
$^{214}_{85}At$	8.8	10.9	11.4	8.99	-6.25	-6.63
$^{216}_{85}At$	8.8	10.95	12.4	7.95	-3.51	-3.82
$^{218}_{85}At$	8.8	11.0	13.5	6.82	0.35	-0.09
$^{204}_{87}Fr$	8.65	10.8	14.0	7.17	0.32	-0.26
$^{206}_{87}Fr$	8.7	10.8	14.2	6.93	1.27	0.61
$^{208}_{87}Fr$	8.7	10.8	14.3	6.77	1.9	1.19
$^{216}_{87}Fr$	8.8	10.95	11.7	9.18	-6.15	-6.44
$^{218}_{87}Fr$	8.8	11.0	12.8	8.01	-3.0	-3.30
$^{220}_{87}Fr$	8.8	11.0	14.0	6.80	1.64	0.83
$^{210}_{89}Ac$	8.7	10.9	13.9	7.60	-0.44	-1.06
$^{212}_{89}Ac$	8.75	10.9	14.0	7.52	-0.02	-0.81
$^{214}_{89}Ac$	8.8	10.9	14.1	7.35	1.46	-0.25
$^{222}_{89}Ac$	8.9	11.0	14.1	7.14	0.65	0.36
$^{222}_{91}Pa$	8.9	11.0	13.4	8.33	-1.94	-2.81
$^{224}_{91}Pa$	8.9	11.1	14.0	7.69	-0.02	-0.79
$^{226}_{91}Pa$	8.9	11.1	14.7	6.99	2.45	1.69
$^{238}_{95}Am$	9.0	11.15	16.4	6.04	9.36	7.58
$^{240}_{95}Am$	9.1	11.2	16.7	5.59	11.05	10.04
$^{242}_{95}Am$	9.1	11.2	16.8	5.59	11.76	10.01
$^{246}_{99}Es$	9.1	11.3	15.5	7.70	3.67	1.97
$^{248}_{99}Es$	9.15	11.3	16.05	7.15	5.75	4.11
$^{252}_{99}Es$	9.2	11.3	16.4	6.74	7.68	5.84
$^{248}_{101}Md$	9.15	11.3	15.1	8.56	1.67	-0.23
$^{256}_{103}Lr$	9.2	11.4	15.35	8.69	1.89	-0.06
$^{258}_{103}Lr$	9.3	11.4	15.1	8.9	0.97	-0.74
$^{260}_{103}Lr$	9.3	11.45	15.6	8.31	2.48	1.15
$^{260}_{105}Db$	9.3	11.3	15.1	9.32	0.45	-1.32

Table 5

	A	**285**	**286**	**287**	**288**	**289**	**290**	**291**	**292**	**293**	**294**	**295**	**296**	**297**	**298**	**299**	**300**	**301**	**302**
-118	Qα	13.3#	13.27#	13.11#	13.11#	12.99#	13.04#	12.79#	12.59#	12.49#	12.51#	12.42#	12.52#	12.34#	12.73#	12.87#	12.94#	13.05#	13.07#
	gldm	-6.91	-6.87	-6.61	-6.63	-6.42	-6.52	-6.06	-5.69	-5.56	-5.60	-5.45	-5.66	-5.32	-6.11	-6.37	-6.51	-6.72	-6.77
	fit	-5.63	-6.35	-5.30	-6.07	-5.09	-5.97	-4.73	-5.09	-4.14	-4.96	-4.02	-5.02	-3.88	-5.49	-5.03	-5.96	-5.42	-6.25
	A	**283**	**284**	**285**	**286**	**287**	**288**	**289**	**290**	**291**	**292**	**293**	**294**	**295**	**296**	**297**	**298**	**299**	**300**
-117	Qα	12.72#	12.64#	12.52#	12.40#	12.31#	12.25#	12.20#	12.14#	11.94#	11.93#	11.91#	11.90#	11.80#	11.59#	11.97#	12.16#	12.25#	12.35#
	gldm	-6.11	-5.96	-5.74	-5.51	-5.36	-5.25	-5.16	-5.05	-4.64	-4.62	-4.64	-4.62	-4.43	-3.98	-4.83	-5.25	-5.44	-5.65
	fit	-5.11	-4.50	-4.74	-3.99	-4.33	-3.69	-4.12	-3.47	-3.58	-3.00	-3.55	-2.96	-3.34	-2.23	-3.76	-3.65	-4.41	-4.13
	A	**280**	**281**	**282**	**283**	**284**	**285**	**286**	**287**	**288**	**289**	**290**	**291**	**292**	**293**	**294**	**295**	**296**	**297**
-116	Qα	12.65#	12.39#	11.90#	12.03#	11.83#	11.68#	11.65#	11.52#	11.55#	11.50#	11.34#	11.33#	11.03#	11.15#	11.19#	11.06#	11.33#	11.38#
	gldm	-6.16	-5.67	-4.72	-5.01	-4.59	-4.27	-4.22	-3.96	-4.04	-3.94	-3.58	-3.57	-2.85	-3.19	-3.30	-3.00	-3.67	-3.80
	fit	-5.61	-4.35	-4.04	-3.61	-3.92	-2.86	-3.54	-2.52	-3.35	-2.51	-2.89	-2.14	-2.16	-1.74	-2.60	-1.55	-2.97	-2.36
	A	**278**	**279**	**280**	**281**	**282**	**283**	**284**	**285**	**286**	**287**	**288**	**289**	**290**	**291**	**292**	**293**	**294**	**295**
-115	Qα	12.90#	12.50#	12.24#	11.80#	11.02#	10.30#	10.56#	10.55#	10.45#	10.48#	10.34#	10.24#	10.15#	9.88#	9.75#	9.69#	9.46#	9.87#
	gldm	-6.85	-6.14	-5.65	-4.74	-3.01	-1.13	-1.85	-1.83	-1.58	-1.68	-1.32	-1.05	-0.80	-0.03	0.35	0.49	1.19	-0.08
	fit	-5.63	-5.21	-4.22	-3.73	-1.25	-0.02	-0.02	-0.74	0.26	-0.59	0.54	0.03	1.07	1.03	2.28	1.56	3.20	0.99
	A	**275**	**276**	**277**	**278**	**279**	**280**	**281**	**282**	**283**	**284**	**285**	**286**	**287**	**288**	**289**	**290**	**291**	**292**
-114	Qα	12.67 #	12.55#	12.55#	12.86#	12.27#	11.83	11.15#	10.22#	9.79#	9.64 #	9.55#	9.61#	9.53 #	9.39#	9.08#	8.73 #	8.66#	8.47#
	gldm	-6.69	-6.47	-6.48	-7.05	-5.97	-5.09	-3.58	-1.22	0.00	0.44	0.71	0.51	0.74	1.16	2.16	3.35	3.59	4.28
	fit	-5.46	-5.94	-5.25	-6.60	-4.71	-4.49	-2.22	-0.54	1.38	1.10	2.07	1.16	2.10	1.80	3.49	3.95	4.90	4.85
	A	**273**	**274**	**275**	**276**	**277**	**278**	**279**	**280**	**281**	**282**	**283**	**284**	**285**	**286**	**287**	**288**	**289**	**290**
-113	Qα	12.31#	12.20#	12.12#	12.11#	12.37#	12.77#	12.83#	11.67#	10.90#	10.00#	9.56 #	9.36#	9.18#	9.10#	9.04#	8.97#	8.66#	9.13#
	gldm	-6.25	-6.05	-5.90	-5.89	-6.41	-7.15	-7.29	-5.05	-3.29	-0.93	0.35	0.96	1.53	1.78	1.96	2.18	3.24	1.63
	fit	-5.33	-4.73	-4.97	-4.56	-5.53	-6.04	-6.50	-3.60	-2.27	0.87	1.39	2.87	2.54	3.72	2.97	4.15	4.23	3.55
	A	**270**	**271**	**272**	**273**	**274**	**275**	**276**	**277**	**278**	**279**	**280**	**281**	**282**	**283**	**284**	**285**	**286**	**287**
-112	Qα	12.30#	12.07#	11.82#	11.72#	11.61#	11.70#	12.05#	12.30#	12.49#	12.03#	11.34#	10.35#	9.62#	9.22#	8.89#	8.80#	8.68#	8.62#
	gldm	-6.41	-5.97	-5.54	-5.34	-5.12	-5.33	-6.05	-6.55	-6.92	-6.06	-4.61	-2.20	-0.16	1.06	2.13	2.43	2.84	3.03
	fit	-5.94	-4.79	-4.96	-4.07	-4.53	-4.06	-5.53	-5.38	-6.48	-4.85	-4.03	-0.89	0.46	2.36	2.73	3.70	3.41	4.29

=111	A	**268**	**269**	**270**	**271**	**272**	**273**	**274**	**275**	**276**	**277**	**278**	**279**	**280**	**281**	**282**	**283**	**284**	**285**
	Qα	12.10#	11.84#	11.54#	11.21#	10.98	11.09#	11.07#	11.53#	11.73#	11.71#	11.59#	11.12#	10.34#	9.58#	9.00#	8.29#	8.22#	8.09#
	gldm	-6.28	-5.77	-5.16	-4.44	-3.98	-4.25	-4.21	-5.26	-5.69	-5.66	-5.42	-4.41	-2.48	-0.34	1.42	3.89	4.14	4.63
	fit	-5.10	-4.90	-3.84	-3.52	-2.47	-3.27	-2.75	-4.33	-4.40	-4.77	-4.10	-3.45	-0.89	0.61	3.28	4.86	6.16	5.58
=110	A	**265**	**266**	**267**	**268**	**269**	**270**	**271**	**272**	**273**	**274**	**275**	**276**	**277**	**278**	**279**	**280**	**281**	**282**
	Qα	12.10#	11.99#	11.78	11.67	11.28	11.17	10.90	10.77	11.67	10.72#	10.92#	10.93#	10.89#	10.61#	9.89#	9.25#	8.75#	7.95#
	gldm	-6.53	-6.33	-5.92	-5.71	-4.88	-4.65	-4.05	-3.79	-5.82	-3.69	-4.18	-4.22	-4.13	-3.46	-1.56	0.33	1.95	4.81
	fit	-5.40	-5.84	-4.76	-5.20	-3.68	-4.10	-2.82	-3.18	-4.63	-3.10	-2.94	-3.65	-2.90	-2.90	-0.33	0.87	3.14	5.35
$_{09}$Mt	A	**263**	**264**	**265**	**266**	**267**	**268**	**269**	**270**	**271**	**272**	**273**	**274**	**275**	**276**	**277**	**278**	**279**	**280**
	Qα	11.87#	11.56#	11.33	11.49	10.98	10.70	10.54	10.35	10.14	9.62#	10.02#	10.26#	10.26#	10.11#	10.04#	9.58#	9.13#	8.65#
	gldm	-6.34	-5.72	-5.25	-5.60	-4.49	-3.84	-3.46	-2.99	-2.44	-1.03	-2.16	-2.83	-2.85	-2.46	-2.28	-0.98	0.36	1.93
	fit	-5.50	-4.50	-4.35	-4.38	-3.57	-2.43	-2.53	-1.52	-1.52	0.58	-1.24	-1.34	-1.92	-0.95	-1.36	0.60	1.26	3.70
$_{08}$Hs	A	**260**	**261**	**262**	**263**	**264**	**265**	**266**	**267**	**268**	**269**	**270**	**271**	**272**	**273**	**274**	**275**	**276**	**277**
	Qα	10.85#	11.04#	11.09#	10.67	10.58	10.47	10.21	10.12	9.90	9.74	8.88#	9.02#	9.39#	9.61#	9.65#	9.58#	9.52#	8.93#
	gldm	-4.36	-4.80	-4.96	-4.01	-3.81	-3.55	-2.90	-2.67	-2.09	-1.65	0.96	0.50	-0.70	-1.36	-1.49	-1.30	-1.13	0.67
	fit	-3.83	-3.67	-4.43	-2.82	-3.26	-2.35	-2.34	-1.48	-1.54	-0.48	1.46	1.63	-0.16	-0.18	-0.96	-0.13	-0.62	1.81
$_{07}$Bh	A	**258**	**259**	**260**	**261**	**262**	**263**	**264**	**265**	**266**	**267**	**268**	**269**	**270**	**271**	**272**	**273**	**274**	**275**
	Qα	10.00#	10.07#	10.34	10.57	10.22	10.08	9.98	9.77	9.56	9.38	8.48#	8.32#	8.36#	8.85#	9.08#	9.02#	8.89#	9.00#
	gldm	-2.53	-2.73	-3.44	-4.02	-3.18	-2.83	-2.58	-2.02	-1.44	-0.92	1.95	2.50	2.35	0.68	-0.11	0.06	0.46	0.10
	fit	-1.10	-1.83	-2.09	-3.16	-1.80	-1.94	-1.16	-1.13	0.05	-0.04	3.64	3.35	4.05	1.52	1.48	0.94	2.08	0.97
$_{06}$Sg	A	**255**	**256**	**257**	**258**	**259**	**260**	**261**	**262**	**263**	**264**	**265**	**266**	**267**	**268**	**269**	**270**	**271**	**272**
	Qα	10.08#	9.72#	9.59#	9.68	9.84	9.93	9.81	9.61	9.39	9.22	8.76	8.76	8.04#	7.77#	7.92#	8.35#	8.59	8.57#
	gldm	-3.02	-2.07	-1.72	-1.99	-2.45	-2.70	-2.39	-1.86	-1.24	-0.76	0.67	0.66	3.15	4.17	3.59	2.00	1.17	1.17
	fit	-1.89	-1.54	-0.59	-1.47	-1.32	-2.19	-1.28	-1.35	-0.12	-0.25	1.78	1.14	4.22	4.62	4.64	2.45	2.23	1.66
$_{05}$Db	A	**253**	**254**	**255**	**256**	**257**	**258**	**259**	**260**	**261**	**262**	**263**	**264**	**265**	**266**	**267**	**268**	**269**	**270**
	Qα	9.97#	9.85#	9.72	9.48	9.32	9.55	9.65	9.32	9.23	9.00	8.83	8.67	8.49	7.54#	7.27#	7.37#	7.76#	8.02#
	gldm	-3.04	-2.73	-2.38	-1.74	-1.28	-1.96	-2.26	-1.32	-1.07	-0.41	0.11	0.61	1.19	4.70	5.82	5.39	3.80	2.81
	fit	-2.18	-1.40	-1.54	-0.34	-0.44	-0.59	-1.42	0.09	-0.25	1.07	0.95	2.15	2.02	6.49	6.61	7.20	4.59	4.45
$_{04}$Rf	A	**250**	**251**	**252**	**253**	**254**	**255**	**256**	**257**	**258**	**259**	**260**	**261**	**262**	**263**	**264**	**265**	**266**	**267**
	Qα	9.94#	9.72#	9.72#	9.55	9.38	9.25	8.95	9.15	9.33	9.12	8.90	8.60	8.50	8.31	8.14	7.17#	6.91#	7.02#
	gldm	-3.23	-2.66	-2.67	-2.23	-1.76	-1.39	-0.51	-1.13	-1.68	-1.07	-0.40	0.55	0.82	1.46	2.04	5.85	7.00	6.49
	fit	-2.75	-1.60	-2.20	-1.17	-1.28	-0.34	-0.05	-0.09	-1.22	-0.03	0.03	1.56	1.28	2.49	2.48	6.84	7.38	7.46

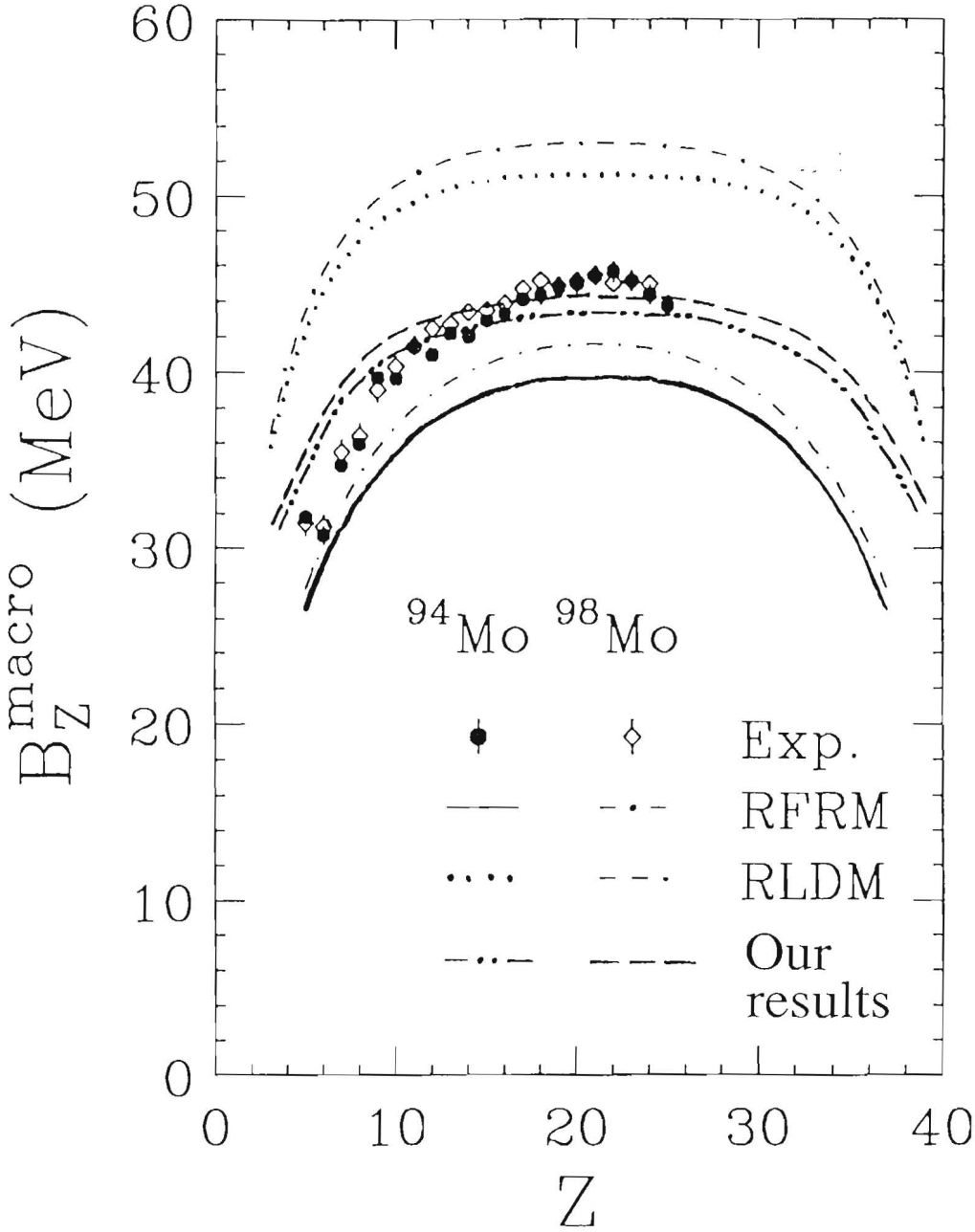
60
50
40
30
20
10
0
0
10
20
30
40
Z
B_Z^{macro} (MeV)
^{94}Mo ^{98}Mo
Exp.
RFRM
RLDM
Our results

Figure 1

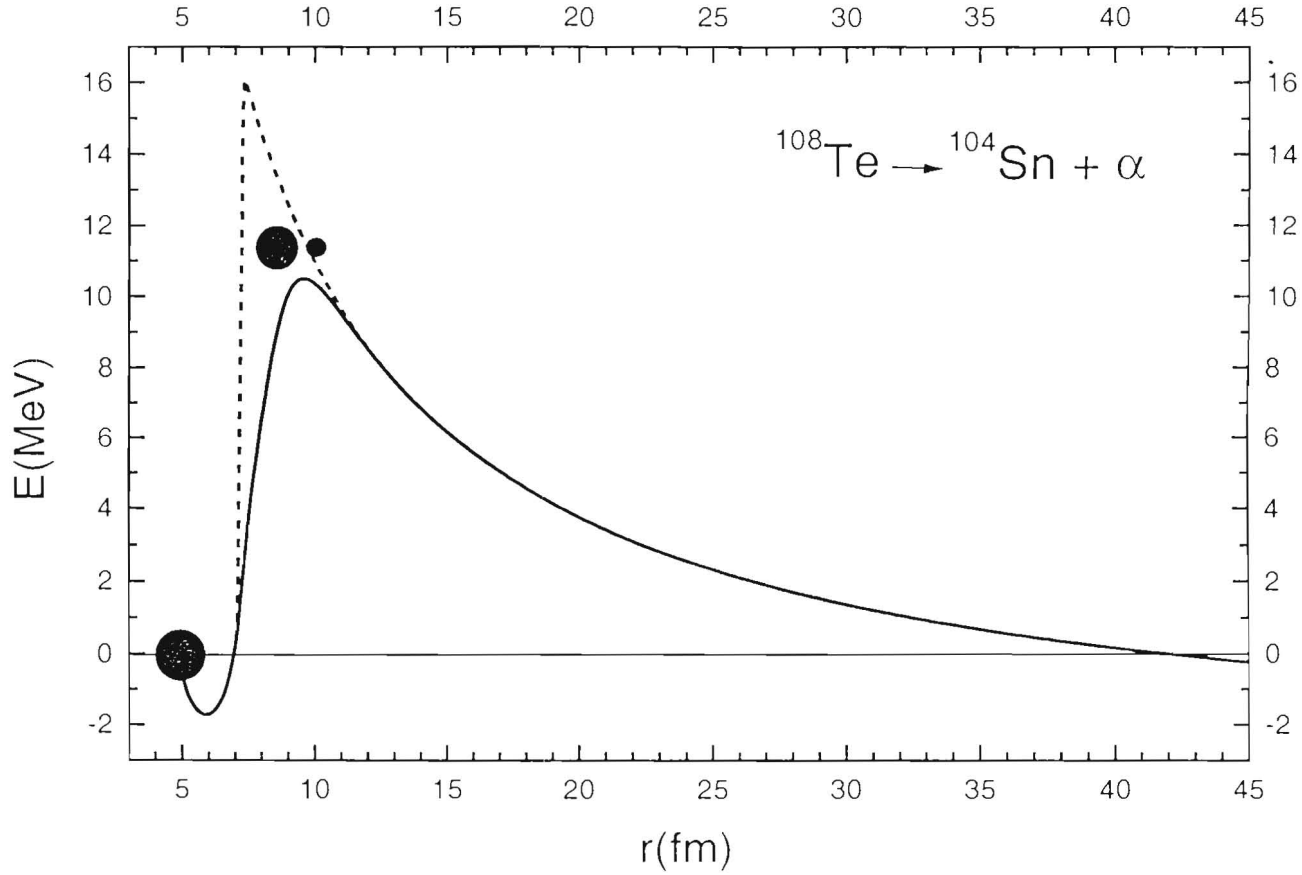

Figure 2

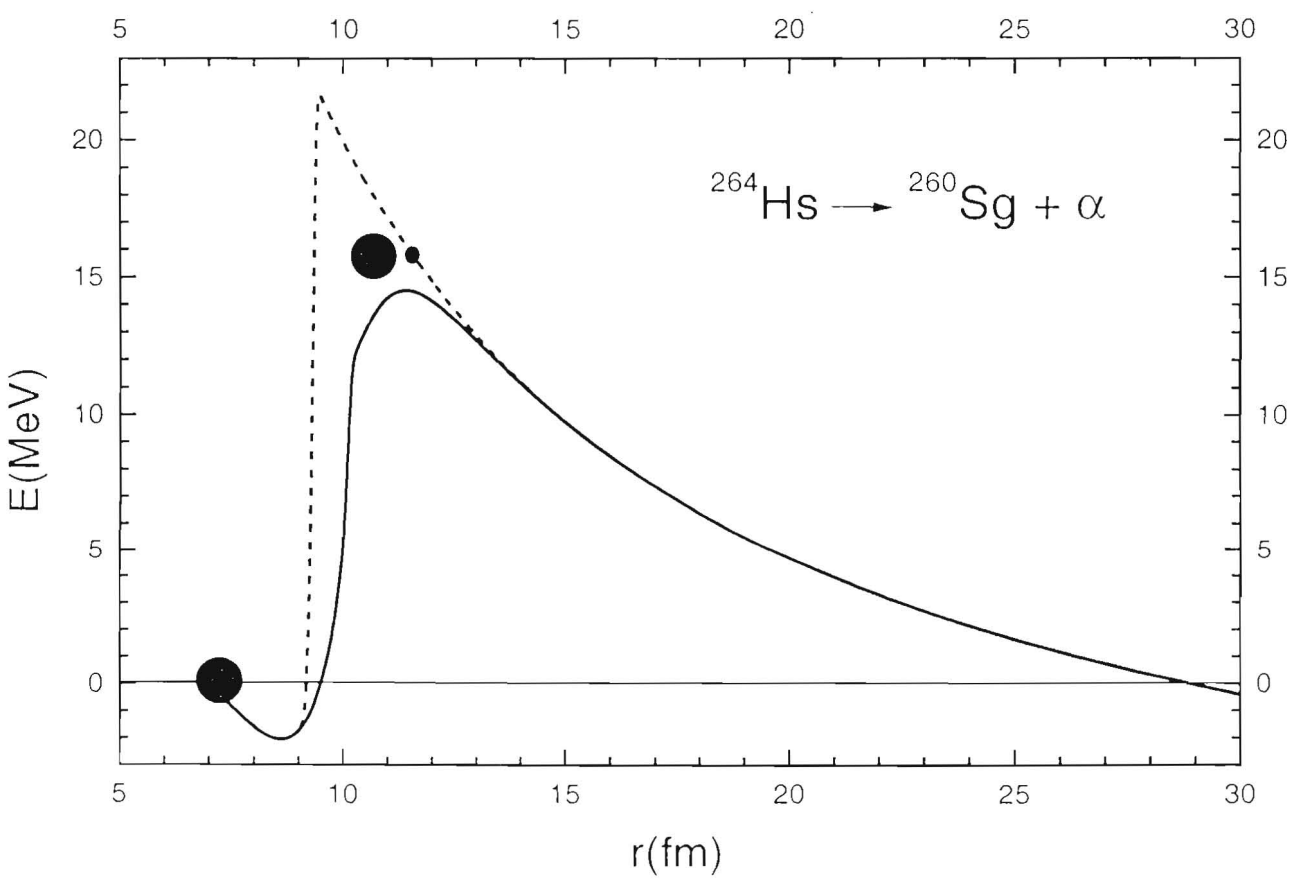

Figure 3